7318 *Macromolecules* **2009**, *42*, 7318–7323
DOI: 10.1021/ma9008669

Macromolecules
ARTICLE

Mechanistic Studies of Photoinitiated Free Radical Polymerization Using a Bifunctional Thioxanthone Acetic Acid Derivative as Photoinitiator

Feyza Karasu,[†] Nergis Arsu,*[,†] Steffen Jockusch,*[,‡] and Nicholas J. Turro[‡]

[†]*Department of Chemistry, Yildiz Technical University, Davutpasa Campus, Istanbul 34210, Turkey, and*
[‡]*Department of Chemistry, Columbia University, 3000 Broadway, New York, New York 10027*

Received April 20, 2009; Revised Manuscript Received August 4, 2009

ABSTRACT: A bifunctional photoinitiator for free radical polymerization, thioxanthone catechol-*O*,*O*′-diacetic acid, was synthesized, characterized, and compared to photoinitiator parameters of the monofunctional analogue, 2-(carboxymethoxy)thioxanthone. Photophysical studies such as fluorescence, phosphorescence, and laser flash photolysis in addition to photopolymerizations of methyl methacrylate show that the bifunctional photoinitiator is more efficient in polymer generation than the monofunctional derivative. These studies suggest that initiator radicals are generated from a $\pi-\pi^*$ triplet state in an intramolecular electron transfer, followed by proton transfer and decarboxylation to generate alkyl radicals, which initiate polymerization. The initial electron transfer is faster for the bifunctional photoinitiator than the monofunctional derivative, which is based on laser flash photolysis studies. Because of the relatively fast intramolecular radical generation from the triplet state (triplet lifetime = 490 ns), quenching by molecular oxygen is insignificant and polymerization of methyl methacrylate proceeds efficiently without deoxygenation. At higher concentrations of initiator (~5 mM) intermolecular electron transfer competes with intramolecular electron transfer. Both processes, inter- and intramolecular processes, yield initiating alkyl radicals.

Introduction

Photoinduced free radical polymerization has found many industrial applications for coatings on various materials.[1−3] One of the most important components in the coating formulation is the photoinitiator, which generates free radicals upon absorption of UV light. Photoinitiated free radical polymerization may be initiated by type I or type II initiators. Most type I photoinitiators form initiating free radicals by α-cleavage of ketones from photoexcited triplet states.[4,5] Type II photoinitiators are based on compounds, mostly aromatic ketones, whose triplet excited states react with hydrogen donors under H-abstraction or electron donors to produce initiating radicals.[6,7] Because the type II initiation is based on bimolecular reaction, they are generally slower than type I photoinitiators, which are based on unimolecular formation of radicals.

Previously, we reported on acetic acid derivatives of thioxanthone, which are single-component photoinitiators (Chart 1).[8,9] Early mechanistic studies on two-component systems of this type suggested an aromatic carbonyl sensitized decarboxylation mechanism. According to Davidson and co-workers,[10,11] excited aromatic carbonyl compounds such as benzophenone can undergo electron transfer with sulfur- or oxygen-containing carboxylic acids to give carboxylate radicals. Subsequent decarboxylation of this radical produces an alkyl radical (Scheme 1). A similar mechanism was proposed to be operative for our single-component initiators (Chart 1), and this mechanism involved intramolecular electron transfer followed by hydrogen abstraction and decarboxylation.[8,9]

Multifunctional initiators are characterized by the presence of at least two (different or identical) functional groups. The primary advantages of multifunctional initiators are higher rates of production of high molecular weight polymers and the generation of polymers of specific compositional structure.[12,13] In this study, as a continuing interest in developing novel photoinitiators, thioxanthone catechol-*O*,*O*′-diacetic acid (TX-Ct) was synthesized and tested as novel single-component bifunctional photoinitiator for free radical polymerization of acrylate monomers (Chart 2). For comparison, the monofunctional analogue TX-Ma was also investigated. Photophysical studies gave further insight into the mechanism of radical generation.

Experimental Section

Materials. Thiosalicylic acid (97%, Aldrich) and catechol-*O*,*O*′-diacetic acid (97%, Alfa-Aesar) and sulfuric acid (H_2SO_4, 98%, Merck) were used as received. Methyl methacrylate (MMA, 99%, Merck) was washed with 5% aqueous NaOH solution, dried over $CaCl_2$, and distilled from CaH_2 in vacuo. *N*,*N*′-Dimethylformamide (DMF, 99%, Merck) was distilled from CaH_2 under reduced pressure. Ethanol (HPLC grade, Aldrich), acetonitrile (HPLC grade, Aldrich), and 2-methyltetrahydrofuran (>99%, Aldrich) were used as received.

Synthesis of (3-Carboxymethoxy-9-oxo-9*H*-thioxanthen-2-yloxy)acetic Acid (Thioxanthone−Catechol-*O*,*O*′-diacetic Acid; TX-Ct). Thiosalicylic acid (0.32 g, 2.0 mmol) was slowly added to concentrated sulfuric acid (15 mL) in an ice bath, and the mixture was stirred for 5 min to ensure thorough mixing. Catechol-*O*,*O*′-diacetic acid (1.35 g, 6.0 mmol) was added slowly to the stirred mixture over a period of 30 min. After the addition, the reaction mixture was stirred at room temperature for 3 days, after which it was left to stand at room temperature overnight. The resulting mixture was poured carefully with stirring into cold water, and a yellow product was obtained (Scheme 2). Yield: 80%; mp: 210 °C. Elemental Anal. Calcd for $C_{17}H_{12}O_7S$ (360 g mol^{-1}): C, 56.66%; H, 3.36%; S, 8.90%. Found: C, 55.84%; H, 3.54%; S, 9.09%. ^{1}H NMR (DMSO, 250 MHz) δ ppm: 4.87 (s, 2H, CH_2), 4.96 (s, 2H, CH_2), 7.37 (s, 1H, aromatic), 7.53−7.59 (m, 1H, aromatic), 7.70−7.76 (m, 1H, aromatic) 7.80−7.84 (m, 2H, aromatic) 8.42−8.46 (d, j: 7.9 Hz, 1H, aromatic), 13.21 (brs, 2H, OH). ^{13}C NMR (DMSO, 50 MHz) δ ppm: 177.28 (C=O), 169.75 (C=O), 169.30 (C=O), 151.85

---

*To whom correspondence should be addressed.

Scheme 1. Bimolecular Radical Generation

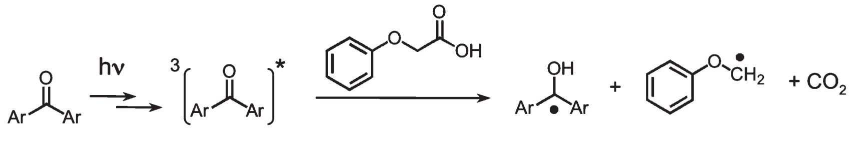

Scheme 2. Synthesis of Thioxanthone−Catechol-*O*,*O*′-diacetic Acid (TX-Ct)

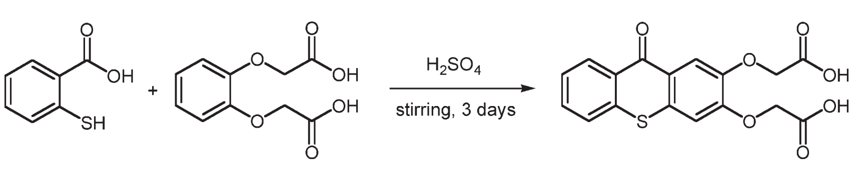

TX-Ct

Chart 1. Structure of Thioxanthone Acetic Acid Derivatives

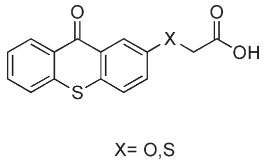

Chart 2. Structures of Investigated Photoinitiators

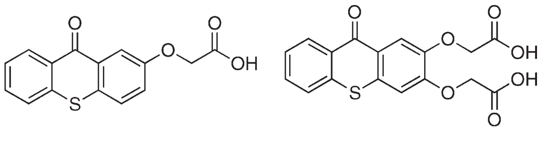

TX-Ma TX-Ct

(Cq), 146.80 (Cq), 136.38 (Cq), 132.28 (Cq), 130.80 (Cq), 128.78 (Cq), 127.66 (CH, Ph), 126.52 (CH, Ph), 126.36(CH, Ph), 122.15 (CH, Ph), 111.18 (CH, Ph), 109.02 (CH, Ph), 65.05 (CH_2), 64.98 (CH_2). IR (KBr): 3413, 2923, 1732, 1717, 1593, 743 cm^{-1}.

Synthesis of 2-(Carboxymethoxy)thioxanthone (TX-Ma). TX-Ma was synthesized as described previously.[8]

Photopolymerization. *Typical Procedure*. A solution of 0.18 mg (5.0×10^{-7} mol) of TX-Ct in 0.5 mL of DMF was added to 0.5 mL (4.68 mmol) of MMA. The solution was put into a Pyrex tube and irradiated for 15 min in an air atmosphere using a photoreactor consisting of a 400 W medium-pressure mercury lamp (light intensity: 435 W/m^2) and a water cooling system. Poly(methyl methacrylate) formed at the end of irradiation was precipitated in 10-fold excess methanol and dried in vacuo (yield: 2.5%; M_n: 32 200 g/mol). All the other polymerizations using different concentrations and additives were performed under identical experimental conditions unless otherwise stated. For the experiments under nitrogen atmosphere, the solutions inside the Pyrex tube were flushed with dry nitrogen prior irradiation. Polymerization yields were calculated for all samples gravimetrically.

Analysis. Gel permeation chromatography (GPC) measurements were performed at room temperature with a setup consisting of a pump (Agilent 1100), a refractive index detector (Agilent 1100s), and three high-resolution Zorbax PSM columns (60S, 300S, and 1000S; size: 6.2 × 250 mm; particle size: 5 μm). The effective molecular weight ranges were 500−10 000, 3000−300 000, and 10 000−1 000 000 g/mol, respectively. Tetrahydrofuran (THF) was used as the eluent (flow rate 0.3 mL/min). The number-average of molecular weight (M_n) was determined using polystyrene standards. ^1H NMR and ^{13}C NMR spectra were recorded on a Bruker-AC-250 or Bruker-AC-200 instrument, respectively, with DMSO as solvent and tetramethylsilane (TMS) as the internal standard. UV−vis spectra were taken on a Varian UV−Visible Cary 50 spectrophotometer. Fluorescence and phosphorescence measurements were performed on a FluoroMax P3 fluorometer (HORIBA Jobin Yvon). Fluorescence lifetimes were measured by time-correlated single photon counting using an OB920 spectrometer (Edinburgh Analytical Instruments) in conjunction with a pulsed light emitting diode (335 nm) as excitation source. IR spectra were recorded on a Perkin-Elmer Spectrum One FT-IR spectrometer on KBr disks. Laser flash photolysis experiments employed the pulses from a Spectra Physics GCR-150-30 Nd: YAG laser (355 nm, ca. 5 mJ/pulse, 5 ns) and a computer-controlled system that has been described elsewhere.[14]

Results and Discussion

The mono- and bifunctional photoinitiators, TX-Ma and TX-Ct, were synthesized by a modified literature procedure according to Scheme 2.[8,15] The absorption spectra of TX-Ct and TX-Ma are shown in Figure 1. TX-Ct possesses absorption characteristics similar to the monofunctional TX-Ma and the parent thioxanthone (Figure 1). The introduction of the second carboxymethoxy group at the 3-position (TX-Ct) causes a slight increase in extinction coefficient but also a slight hypsochromic shift (compared to TX-Ma). However, the high molar absorptivities (~4000 M^{-1} cm^{-1}) of both TX-Ct and TX-Ma ensure effective light absorption in the near-UV spectral region. Additional photophysical parameters are summarized in Table 1. TX-Ct and TX-Ma show fluorescence (Figure 2) with relatively high quantum yields in the protic ethanol (0.28 and 0.35, respectively) compared to the unsubstituted thioxanthone (0.07 in ethanol).[16] These high fluorescence quantum yields reduce the triplet yield, the state from which initiator radicals are generated. However, in the nonprotic solvent 2-methyltetrahydrofuran the fluorescence quantum yields are significantly lower (0.013 and 0.026 for TX-Ct and TX-Ma, respectively), which is consistent with reported solvent effects on the fluorescence quantum yields[18] and triplet quantum yields.[19] The solvent dependence of the fluorescence quantum yields is also directly reflected in the fluorescence lifetimes (Table 1). For example, TX-Ct shows in the protic solvent ethanol a relatively long fluorescence lifetime (5.7 ns) and high fluorescence quantum yield (0.28), whereas in the nonprotic solvent 2-methyltetrahydrofuran the fluorescence lifetime is short (< 0.2 ns) and the fluorescence quantum yield is low (0.013).

Phosphorescence measurements at 77 K were performed to gain information on the triplet energies and electron configuration of the triplet states (Figure 2). Phosphorescence spectra of ketones with n−π* nature of the lowest triplet state are usually structured, due to the vibrational progression of the C=O vibration, and π−π* triplets are mostly unstructured.[20,21] In addition, phosphorescence lifetimes for n−π* triplets are significantly shorter (on the order of several milliseconds) compared to π−π* triplets (more than 100 ms).[22,22] Therefore, the broad

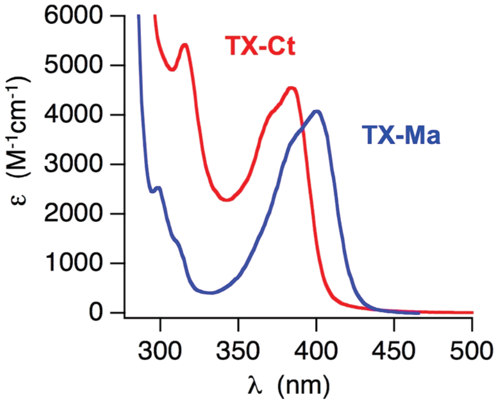

Figure 1. UV-absorption spectra (molar absorptivity) of 2-(carboxymethoxy)thioxanthone (TX-Ma) and thioxanthone−catechol-*O*,*O*′-diacetic acid (TX-Ct) in *N*,*N*′-dimethylformamide (0.25 mM).

Table 1. Photophysical Properties of Thioxanthone−Catechol-*O*, *O*′-diacetic Acid (TX-Ct) and 2-(Carboxymethoxy)thioxanthone (TX-Ma)

	TX-Ct	TX-Ma
ε (M^{-1} s^{-1}) [λ_{max}][a]	4540 [384 nm]	4070 [400 nm]
E^S (kJ/mol)[b]	294	279
E^T (kJ/mol)[c]	257 (EtOH), 253 (Me-THF)	246 (EtOH), 243 (Me-THF)
Φ_f[d]	0.28 (EtOH), 0.013 (Me-THF)	0.35 (EtOH), 0.026 (Me-THF)
τ_f (ns)[e]	5.7 (EtOH), < 0.2 (Me-THF)	9.3 (EtOH), < 0.4 (Me-THF)
τ_p (ms)[f]	144 (EtOH), 171 (Me-THF)	154 (EtOH), 208 (Me-THF)
τ_t (ns)[g]	490	750

[a] Molar absorptivity in *N*,*N*′-dimethylformamide, error limit 5%. [b] Singlet energy determined from fluorescence excitation and emission spectra in ethanol, error limit 2 kJ/mol. [c] Triplet energy determined from phosphorescence spectra in ethanol (EtOH) glass or 2-methyltetrahydrofuran (Me-THF) glass at 77 K, error limit 4 kJ/mol. [d] Fluorescence quantum yield (error limit 15%) using 9,10-diphenylanthracene as standard.[17] [e] Fluorescence lifetime at room temperature, error limit 4%. [f] Phosphorescence lifetime at 77 K, error limit 10%. [g] Triplet lifetime in acetonitrile at room temperature, error limit 4%.

unstructured phosphorescence spectra (Figure 2) together with the long phosphorescence lifetimes at 77 K (144 ms for TX-Ct and 154 ms for TX-Ma in ethanol) indicate a $\pi-\pi^*$ nature of the lowest triplet state.

Laser flash photolysis experiments were performed to investigate the triplet states and their reactivities. Figures 3a and 4a show the transient absorption spectra of TX-Ma and TX-Ct directly after laser excitation. Two transient absorption maxima were observed at 320−330 and 620−630 nm. Both transients were quenched by molecular oxygen with rate constants of ~5 × 10^9 M^{-1} s^{-1} (see Supporting Information) consistent with a triplet or radical nature of the transients. The transient absorptions at ~625 nm (Figures 3c and 4c) decayed monoexponentially with lifetimes of 750 and 490 ns for TX-Ma and TX-Ct, respectively. These transients were assigned to the triplet−triplet absorption of these TX derivatives based on similarities with triplet−triplet absorption spectra of other TX derivatives.[9,18,23,24] The transient absorptions at 320−330 nm (Figures 3b and 4b) showed complex kinetics and are probably caused by an overlap of triplet−triplet absorption and ketyl radical absorption.

Typically, triplet states of thioxanthone and its derivatives show lifetimes longer than 20 μs.[7] However, relatively short triplet lifetimes of 750 and 490 ns for TX-Ma and TX-Ct, respectively, were observed. Previously, we observed an even short triplet lifetime (65 ns) for a similar thioxanthone derivative (Chart 1, X = S).[9] We explained this short triplet lifetime with an intramolecular electron transfer followed by decarboxylation. A similar intramolecular mechanism is also proposed for TX-Ma and TX-Ct (Scheme 3). Because of the low concentration of the thioxantone derivatives in these laser flash photolysis experiments (~10^{-4} M), the reaction is expected to occur intramolecularly and not intermolecularly (Scheme 3).

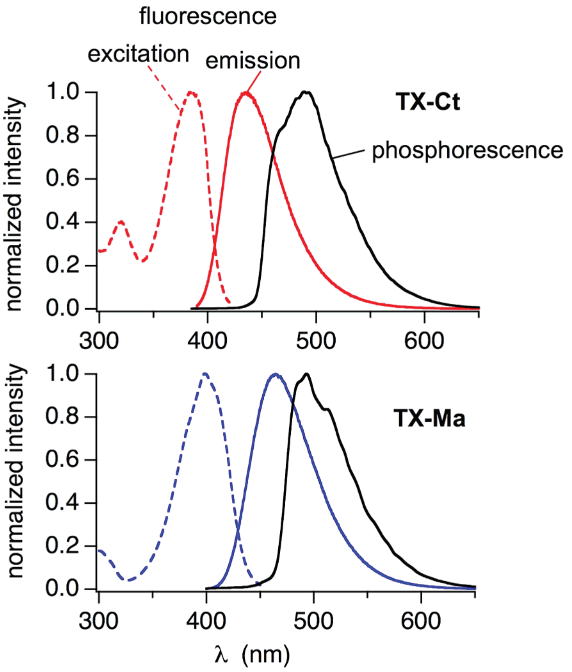

Figure 2. Fluorescence excitation (dashed lines) and emission (blue and red solid lines) spectra of ethanol solutions of thioxanthone−catechol-*O*,*O*′-diacetic acid (TX-Ct) (top; 35 μM) and 2-(carboxymethoxy)thioxanthone (TX-Ma) (bottom; 50 μM) at room temperature. Time-resolved phosphorescence spectra (black solid lines) of TX-Ct (top; 0.23 mM) and TX-Ma (bottom; 0.33 mM) in ethanol glass at 77 K recorded from 0.01 to 10 ms after the excitation pulse.

To demonstrate that decarboxylation occurred, the generated CO_2 was detected in the apparatus shown in the Supporting Information (Figure S1). 1 mL of each solution of TX-Ma and TX-Ct (5 mM) in DMF was placed in a Pyrex tube which was connected to another tube containing an aqueous solution of Na_2CO_3 (0.67 mM) and one drop of phenolphthalein solution (0.025 mM). Under our irradiation conditions (UVA: 12 W/m^2; UVB: 50 W/m^2) the pink color of the phenolphthalein solution disappeared after ~1 h of irradiation of the two photoinitiators, which indicates CO_2 generation.

To test the initiation efficiency of the generated radicals, polymerization experiments of MMA were performed using TX-Ma and TX-Ct as photoinitiators (Table 2). For these polymerization studies, the acrylic monomer, MMA, and varying amounts of photoinitiator were dissolved in DMF and irradiated for 15 min. Irradiation conditions were selected to allow only low conversions of the monomer into the polymer. Low conversions ensure the study of the initiation step more accurately than with high conversions, where gel effects and chain transfer reactions dominate. In general, the bifunctional photoinitiator, TX-Ct, generates more polymer (higher conversions) than the monofunctional TX-Ma in the absence of oxygen (Table 2). Under our experimental conditions, the highest conversions were achieved at initiator concentrations of 2.5 mM. At higher initiator concentrations (5 mM), light penetration problems probably reduce the polymer yield. Even at initiator concentrations as low as 50 μM significant polymerization was still observed.

Another advantage of TX-Ct and TX-Ma is the ability to initiate polymerization under aerobic conditions, which are more attractive for industrial applications. Polymer yields (conversions) and molecular weights (M_n) of the polymer were only slightly reduced compared to deoxygenated samples (Table 2). This is in contrast to most other thioxanthone type II photoinitiator systems, where initiator radicals are formed by hydrogen abstraction of the long-lived thioxanthone triplet from co-initiators, such as amines or thiols. In these type II photoinitiator systems initiation is inhibited due to oxygen quenching of the thioxanthone triplets. Because TX-Ct and TX-Ma can undergo intramolecular reactions to generate initiator radicals in less than 1 μs, oxygen quenching of the triplet states is less of a problem.

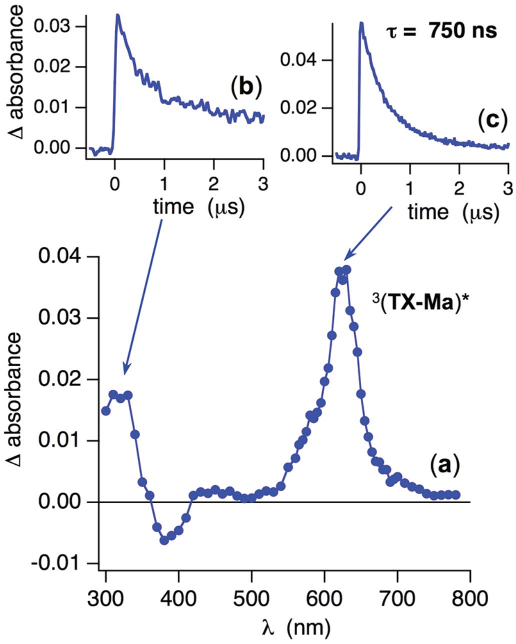

Figure 3. Transient optical absorption spectrum recorded at the end of the laser flash (355 nm, 5 ns) of argon-saturated acetonitrile solutions of 2-(carboxymethoxy)thioxanthone (TX-Ma) (a). The insets show the decay kinetics at 320 nm (b) and 620 nm (c).

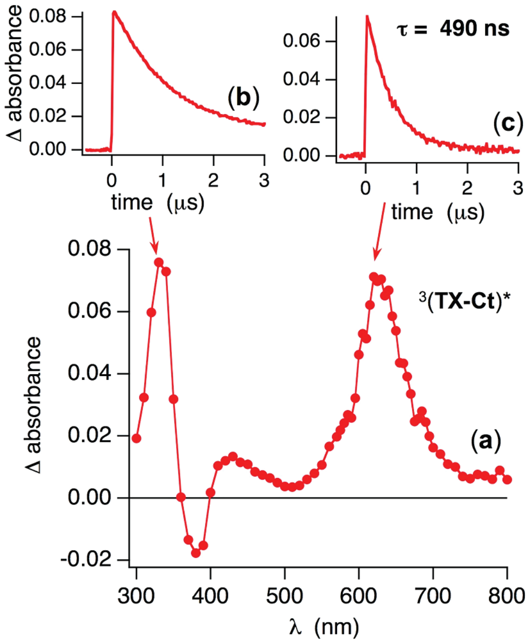

Figure 4. Transient optical absorption spectrum recorded at the end of the laser flash (355 nm, 5 ns) of argon-saturated acetonitrile solutions of thioxanthone–catechol-*O*,*O*′-diacetic acid (TX-Ct) (a). The insets show the decay kinetics at 330 nm (b) and 630 nm (c).

Scheme 3. Proposed Mechanism of Photoinduced Radical Generation and Polymerization

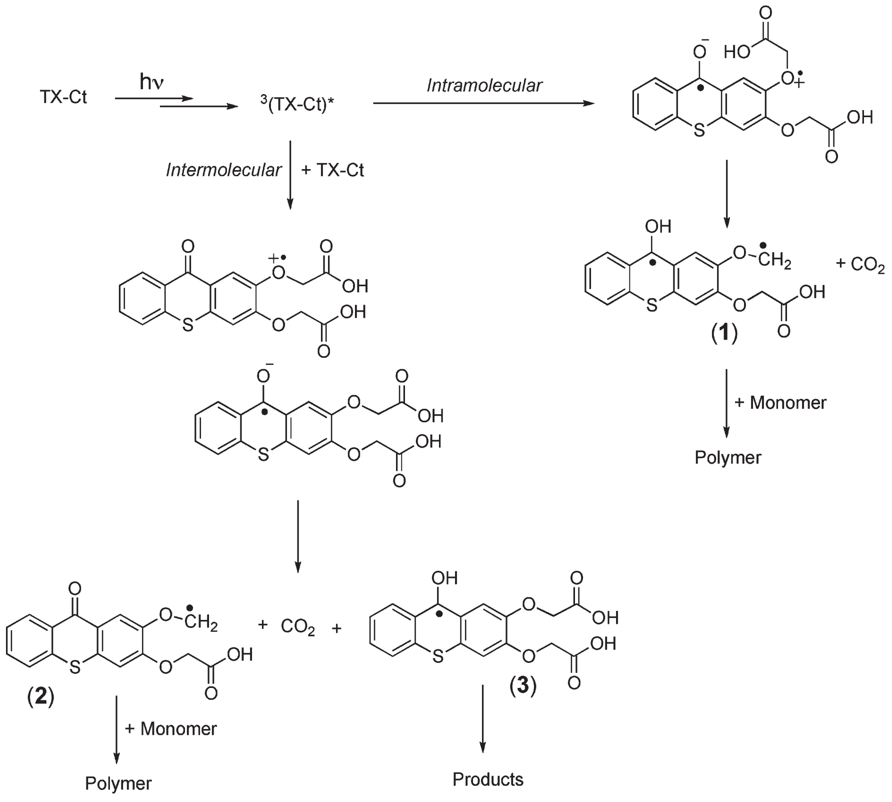

According to Scheme 3, at low initiator concentrations an intramolecular process of radical generation is expected due to the short lifetime of the triplet states (750 and 490 ns for TX-Ma and TX-Ct, respectively). However, at high initiator concentrations (5 mM) intermolecular radical generation involving two initiator molecules could occur. Initiation of polymerization with radical **2** (Scheme 3) leads to incorporation of the TX chromophore into the growing polymer chain. Initiation of polymerization with radical **1** (from intramolecular reaction) should not contain the TX chromophore. UV absorption spectra of purified polymer produced from initiation with a high initiator concentration (5 mM) showed some absorbance at 390 nm, which indicates TX chromophores bound to polymers (Figure 5). However, no absorbance attributed to TX was observed in the case of initiation with a low initiator concentration (0.05 mM) (see Supporting Information).

Table 2. Photoinitiated Polymerization of Methyl Methacrylate (MMA) at 25 °C in *N*,*N*′-Dimethylformamide with 2-(Carboxymethoxy)thioxanthone (TX-Ma) or Thioxanthone−Catechol-*O*,*O*′-diacetic Acid (TX-Ct) as Photoinitiator[a]

		conversion (%)		$M_n \times 10^{-3}$ (g/mol)	
photoinitiator	[photoinitiator] (mM)	N_2	air	N_2	air
TX-Ct	5.0	4.8	3.0	24.8	23.8
	2.5	5.8		25.1	
	0.5	3.9	2.5	35.7	32.2
	0.05	0.8		52.7	
TX-Ma	5.0	2.5	2.5	20.2	22.3
	2.5	2.9		23.7	
	0.5	2.2	3.5	30.9	29.9
	0.05	0.2		51.2	

[a] [MMA] = 4.7 M; irradiation time = 15 min.

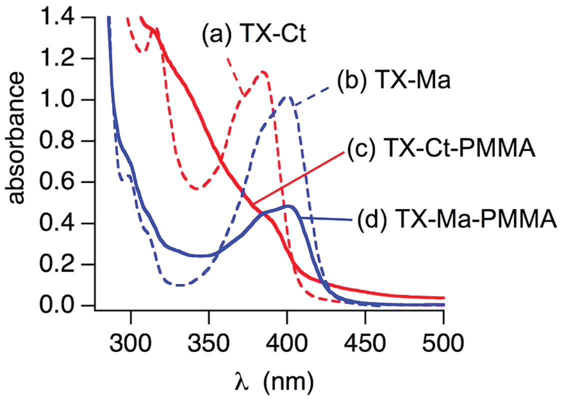

Figure 5. UV absorption spectra (solid lines) of poly(methyl methacrylate) (5 mg/mL) in DMF obtained by photoinitiated polymerization of methyl methacrylate under nitrogen with thioxanthone−catechol-*O*,*O*′-diacetic acid (TX-Ct) (c) and 2-(carboxymethoxy)thioxanthone (TX-Ma) (d) ([PI] = 5 mM). The dashed lines show the absorption spectra of TX-Ct (a) and TX-Ma (b) for comparison.

The purified polymers generated by initiation with a high initiator concentration (5 mM), which contains the TX chromophore, were used as polymeric photoinitiators to polymerize MMA. In the case of the bifunctional photoinitiator (TX-Ct) the resulting polymer was able to initiate further polymerization as reflected by the increase in molecular weight M_n (from 24 800 to 36 400) and MMA conversion of 4.4% (Table 3). However, when the monofunctional TX-Ma was used to generate the initial polymer, this TX-containing polymer showed a significantly lower ability to initiate further polymerization of MMA (Table 3). Only 1.6% of MMA converted into polymer, and the resulting polymer showed only a minor increase in M_n (from 20 200 to 25 800). This observation is consistent with the proposed initiation mechanism, where in the case of the bifunctional photoinitiator a monofunctional polymeric photoinitiator (containing the $-O-CH_2-COOH$ functionality) is generated, which yields initiating radicals upon further photolysis. The increase in the molecular weight of the secondary polymers using the polymeric photoinitiators is demonstrated in Figure 6. For TX-Ct, the peak of the GPC trace of the secondary polymer is shifted to shorter retention times (higher molecular weights) compared to the trace of the initial polymeric initiator. The shoulder at ∼41 min in the trace of the secondary polymer (Figure 6, right) shows that some of the polymeric photoinitiator molecules did not grow in the secondary polymerization step, which is probably caused by inactive polymeric photoinitiator molecules which do not contain the $TX-O-CH_2-COOH$ functionality. In the case that the monofunctional TX-Ma was used to generate the polymeric photoinitiator, the resulting polymer showed a GPC trace with a maximum at the same retention time as the polymeric photoinititor (Figure 6, left),

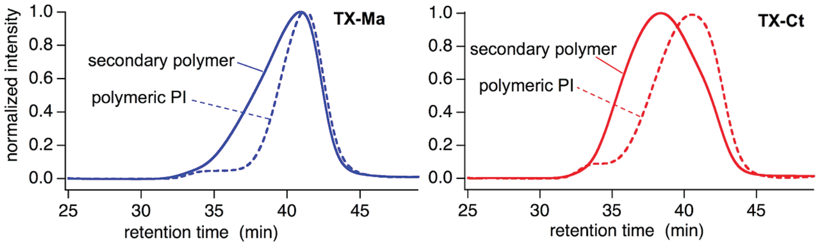

Figure 6. Gel permeation chromatography (GPC) traces of polymeric photoinitiators (dashed lines) obtained by photoinitiated polymerization of methyl methacrylate with 2-(carboxymethoxy)thioxanthone (TX-Ma) (left) and thioxanthone−Catechol-*O*,*O*′-diacetic acid (TX-Ct) (right). GPC traces of the resulting polymers after photopolymerization of methyl methacrylate using the polymeric photoinitiators (solid lines). For further details see Table 3.

Table 3. Photoinitiated Polymerization of Methyl Methacrylate (4.7 M) at 25 °C in *N*,*N*′-Dimethylformamide with Polymeric Photoinitiators (20 mg/mL)[a] **Obtained by Photoinitiated Polymerization of Methyl Methacrylate with 2-(Carboxymethoxy)thioxanthone (TX-Ma) or Thioxanthone−Catechol-*O*,*O*′-diacetic Acid (TX-Ct) as Photoinitiator in the Absence of Oxygen (Irradiation Time 15 min)**

photoinitiator			
type	$M_n \times 10^{-3}$ (g/mol)	conversion (%)	$M_n \times 10^{-3}$ (g/mol)
(TX-Ct)-PMMA	24.8	4.4	36.4
(TX-Ma)-PMMA	20.2	1.6	25.8

[a] This amount corresponds to a concentration of TX chromophores of 0.3−0.5 mM.

which shows that most of the polymeric photoinitiator molecules are inactive.

Conclusions

The photoinitiators TX-Ma and TX-Ct initiate free radical polymerization efficiently. The bifunctional photoinitiator TX-Ct is more efficient in polymer generation than the monofunctional TX-Ma. Photophysical studies, such as fluorescence, phosphorescence, and laser flash photolysis, suggest that initiator radicals are generated in an intramolecular electron transfer, followed by proton transfer and decarboxylation to generate alkyl radicals, which initiate polymerization. The initial electron transfer is faster for the bifunctional TX-Ct than the monofunctional TX-Ma, which is based on laser flash photolysis studies. At higher initiator concentrations, such as 5 mM, intermolecular electron transfer competes with intramolecular electron transfer. However, both processes yield initiating alkyl radicals. Because of the fast intramolecular triplet reaction, inhibition by molecular oxygen is negligible.

Acknowledgment. F.K. and N.A. thank TUBITAK, Yildiz Technical University Research Fund, and the Turkish State Planning Organization (DPT) for financial support. S.J. and N. J.T. thank the National Science Foundation (Grant NSF-CHE-07-17518) for financial support. We thank Prof. Y. Yagci (Istanbul Technical University) for helpful discussions.

Supporting Information Available: Experimental details to measure CO_2, quenching rate constants by O_2, and UV−vis analysis of polymers. This material is available free of charge via the Internet at http://pubs.acs.org.

Note Added after ASAP Publication. This article was published ASAP on September 4, 2009. Table 1 has been modified. The correct version was published on September 10, 2009.

References and Notes

(1) Fouassier, J. P. *Photoinitiation, Photopolymerization and Photocuring*; Hanser Verlag: Munich, 1995.

(2) Dietliker, K. *Chemistry & Technology of UV & EB Formulation for Coatings, Inks & Paints*; SITA Technology Ltd.: London, 1991; Vol. *III*.

(3) Decker, C. *Prog. Polym. Sci* . **1996**, *21*, 593.

(4) Laleveé, J.; Allonas, X.; Jradi, S.; Fouassier, J.-P. *Macromolecules* **2006**, *39*, 1872–1879.

(5) Jockusch, S.; Koptyug, I. V.; McGarry, P. F.; Sluggett, G. W.; Turro, N. J.; Watkins, D. M. *J. Am. Chem. Soc.* **1997**, *119*, 11495–11501.

(6) Davidson, R. S. In *Advances in Physical Chemistry*; Bethel, D., Gold, V., Eds.; Academic Press: London, 1983.

(7) Amirzadeh, G.; Schnabel, W. *Makromol. Chem.* **1981**, *182*, 2821–2835.

(8) Aydin, M.; Arsu, N.; Yagci, Y. *Macromol. Rapid Commun.* **2003**, *24*, 718–723.

(9) Aydin, M.; Arsu, N.; Yagci, Y.; Jockusch, S.; Turro, N. J. *Macromolecules* **2005**, *38*, 4133–4138.

(10) Davidson, R. S.; Harrison, K.; Steiner, P. R. *J. Chem. Soc. C* **1971**, 3480–3482.

(11) Davidson, R. S.; Steiner, P. R. *J. Chem. Soc., Perkin Trans. 2* **1972**, 1357–1362.

(12) Chen, Y.; Loccufier, J.; Vanmaele, L.; Barriau, E.; Frey, H. *Macromol. Chem. Phys.* **2007**, *208*, 1694–1706.

(13) Scorah, M. J.; Dhib, R.; Pendilis, A. *Macromol. React. Eng.* **2007**, *1*, 209–221.

(14) Yagci, Y.; Jockusch, S.; Turro, N. J. *Macromolecules* **2007**, *40*, 4481–4485.

(15) Catalina, F.; Tercero, J. M.; Peinado, C.; Sastre, R.; Mateo, J. L.; Allen, N. S. *J. Photochem. Photobiol. A* **1989**, *50*, 249–258.

(16) Dalton, J. C.; Montgomery, F. C. *J. Am. Chem. Soc.* **1974**, *96*, 6230–6232.

(17) Morris, J. V.; Mahaney, M. A.; Huber, J. R. *J. Phys. Chem.* **1976**, *80*, 969–974.

(18) Abdullah, K. A.; Kemp, T. J. *J. Photochem.* **1986**, *32*, 49–57.

(19) Allonas, X.; Ley, C.; Bibaut, C.; Jacques, P.; Fouassier, J. P. *Chem. Phys. Lett.* **2000**, *322*, 483–490.

(20) Lower, S. K.; El-Sayed, M. A. *Chem. Rev.* **1966**, *66*, 199–236.

(21) Turro, N. J.; Ramamurthy, V.; Scaiano, J. C. *Principles of Molecular Photochemistry: An Introduction*; University Science Books: Sausalito, CA, 2009.

(22) Carmichael, I.; Hug, G. L. In *CRC Handbook of Organic Photochemistry*; Scaiano, J. C., Ed.; CRC Press: Boca Raton, FL, 1989; Vol. *1*, pp 369−403.

(23) Ferreira, G. C.; Schmitt, C. C.; Neumann, M. G. *J. Braz. Chem. Soc.* **2006**, *17*, 905–909.

(24) Neumann, M. G.; Gehlen, M. H.; Encinas, M. V.; Allen, N. S.; Corrales, T.; Peinado, C.; Catalina, F. *J. Chem. Soc., Faraday Trans.* **1997**, *93*, 1517–1521.